



Novel Resectable Myocardial Model Using Hybrid Three-Dimensional Printing and Silicone Molding for Mock Myectomy for Apical Hypertrophic Cardiomyopathy

Wooil Kim¹, Minje Lim², You Joung Jang², Hyun Jung Koo¹, Joon-Won Kang¹,
Sung-Ho Jung³, Dong Hyun Yang¹

Departments of ¹Radiology and Research Institute of Radiology, ³Thoracic and Cardiovascular Surgery, University of Ulsan College of Medicine, Asan Medical Center, Seoul, Korea; ²Anymedi Inc., Seoul, Korea

Objective: We implemented a novel resectable myocardial model for mock myectomy using a hybrid method of three-dimensional (3D) printing and silicone molding for patients with apical hypertrophic cardiomyopathy (ApHCM).

Materials and Methods: From January 2019 through May 2020, 3D models from three patients with ApHCM were generated using the end-diastolic cardiac CT phase image. After computer-aided designing of measures to prevent structural deformation during silicone injection into molding, 3D printing was performed to reproduce anatomic details and molds for the left ventricular (LV) myocardial mass. We compared the myocardial thickness of each cardiac segment and the LV myocardial mass and cavity volumes between the myocardial model images and cardiac CT images. The surgeon performed mock surgery, and we compared the volume and weight of the resected silicone and myocardium.

Results: During the mock surgery, the surgeon could determine an ideal site for the incision and the optimal extent of myocardial resection. The mean differences in the measured myocardial thickness of the model (0.3, 1.0, 6.9, and 7.3 mm in the basal, midventricular, apical segments, and apex, respectively) and volume of the LV myocardial mass and chamber (36.9 mL and 14.8 mL, 2.9 mL and -9.4 mL, and 6.0 mL and -3.0 mL in basal, mid-ventricular and apical segments, respectively) were consistent with cardiac CT. The volume and weight of the resected silicone were similar to those of the resected myocardium (6 mL [6.2 g] of silicone and 5 mL [5.3 g] of the myocardium in patient 2; 12 mL [12.5 g] of silicone and 11.2 mL [11.8 g] of the myocardium in patient 3).

Conclusion: Our 3D model created using hybrid 3D printing and silicone molding may be useful for determining the extent of surgery and planning surgery guided by a rehearsal platform for ApHCM.

Keywords: Apical hypertrophic cardiomyopathy; Mock surgery; Silicone molding; Transapical myectomy; Three-dimensional (3D) printing

INTRODUCTION

Hypertrophic cardiomyopathy (HCM), a genetic myocardial disease characterized by the presence of otherwise unexplainable left ventricular (LV) hypertrophy, has multiple

phenotypic variants [1]. Among these, apical hypertrophic cardiomyopathy (ApHCM), which accounts for 8% of all HCM cases, has been known to have a favorable prognosis; however, recent data suggest associated annual cardiac death rates of 0.5–4%, which are comparable to those

Received: September 25, 2020 **Revised:** September 25, 2020 **Accepted:** December 1, 2020

This research was supported by the Basic Science Research Program, through the National Research Foundation of Korea (NRF), funded by the Ministry of Science, ICT & Future Planning (NRF-2020R1A2C2003843).

Corresponding author: Dong Hyun Yang, MD, Department of Radiology and Research Institute of Radiology, University of Ulsan College of Medicine, Asan Medical Center, 88 Olympic-ro 43-gil, Songpa-gu, Seoul 05505, Korea.

• E-mail: donghyun.yang@gmail.com

This is an Open Access article distributed under the terms of the Creative Commons Attribution Non-Commercial License (<https://creativecommons.org/licenses/by-nc/4.0>) which permits unrestricted non-commercial use, distribution, and reproduction in any medium, provided the original work is properly cited.

of classic HCM [2,3]. The mainstay of management for ApHCM is medical treatment, but for severely symptomatic patients due to small LV end-diastolic volume (LVEDV) or concomitant midventricular obstruction, transapical myectomy to increase end-diastolic dimensions (thereby augmenting LVEDV and increasing stroke volume) is a promising option for symptomatic improvement and potential improvement in survival outcomes [4-8]. However, myectomy is rarely performed for patients with HCM due to various factors. The main factor is the difficult learning curve and the paucity of experienced surgeons and a lack of intra- and inter-observer reliability related to the extent of resection required, which is merely determined by each surgeon's subjective assessment [9,10]. Therefore, to facilitate the widespread use of transapical myectomy for the management of ApHCM, a surgical platform for operative simulation should be useful.

Three-dimensional (3D) printing is increasingly being used in cardiac surgery, especially for complex congenital heart disease [11-13]. Despite the difficulty with quantifying the advantages associated with using 3D printed models in cardiac surgery, surgeons have reported the benefits of individualized surgery planning and training [13-17]. However, the current limitations related to reproducing anatomic details while creating a suitable model that can be manipulated meaningfully by a surgeon are obstacles to applying 3D printing as part of a surgical rehearsal platform. In our experience, the 3D-printed myocardial model for HCM, with the septal myocardium reproduced using the softest material available, was so hard that it was even difficult to apply an incision [18]. On the other hand, considering only the resectability of the model, a simple silicone molding method may be applied [19-21]. However, this method has its limitations because crucial and complex anatomic details, such as the coronary arteries, can be obscured or ignored.

Therefore, we implemented a novel resectable myocardial model for mock myectomy using a hybrid method of 3D printing and silicone molding for ApHCM.

MATERIALS AND METHODS

General Information

Three consecutive patients with ApHCM who underwent myectomy at our institution were enrolled in this study between January 2019 and May 2020. All three patients were diagnosed with HCM by echocardiography and cardiac

CT. They were eligible for surgery and met the following criteria: 1) midventricular obstruction with flow acceleration causing a pressure gradient of ≥ 50 mm Hg at rest or with physiological provocation measured on echocardiography or 2) heart failure symptoms with New York Heart Association (NYHA) functional class III or IV, which was unresponsive to maximum pharmacological therapy. This retrospective study was approved by the institutional review board of Asan Medical Center (Seoul, Korea), which waived the requirement for informed consent from patients.

Process of Developing a Resectable Myocardial Model

The process, involving CT image acquisition and computer-aided design (CAD), for developing a resectable myocardial model is summarized in Figure 1A.

Image Acquisition

A second-generation dual-source CT scanner (Somatom Definition Flash; Siemens) was used to perform electrocardiography (ECG)-gated cardiac CT scanning. Patients with no contraindications to beta-blockers and initial heart rates of > 75 bpm received an oral dose of 2.5 mg bisoprolol (Concor, Merck) 1 hour before the CT examination. A bolus of 70–90 mL of contrast agent was administered using a power injector (Stellant D; Medrad) at a rate of 4.0 mL/s, followed by 40 mL of saline chaser. Retrospective ECG-gated spiral scanning was performed for all the patients, and ECG-based tube current modulation (with a dose pulsing window of 30–80% of the RR interval) was applied for patients without atrial fibrillation. The scan parameters were as follows: tube voltage, 80–120 kV; tube current-exposure time product, 185–380 mAs; collimation, 128 x 0.6 mm; and gantry rotation time, 280 seconds. The mean period between the cardiac CT and surgery was 30.7 days (range, 18–40 days). With a commercially available workstation (Advantage Windows 4.6; GE Healthcare), the cardiac chambers and great vessels were segmented and converted into a standard tessellation language (STL) file format with 3D mesh. Subsequently, the CT images and STL files were transferred to a company (Anymedi Inc.) for CAD and printing.

CAD

CAD of the myocardial model was performed using commercially available software (Materialise 3-matic; Materialise). The segmented areas of the original STL files from the CT data were the coronary artery, left atrium (LA)

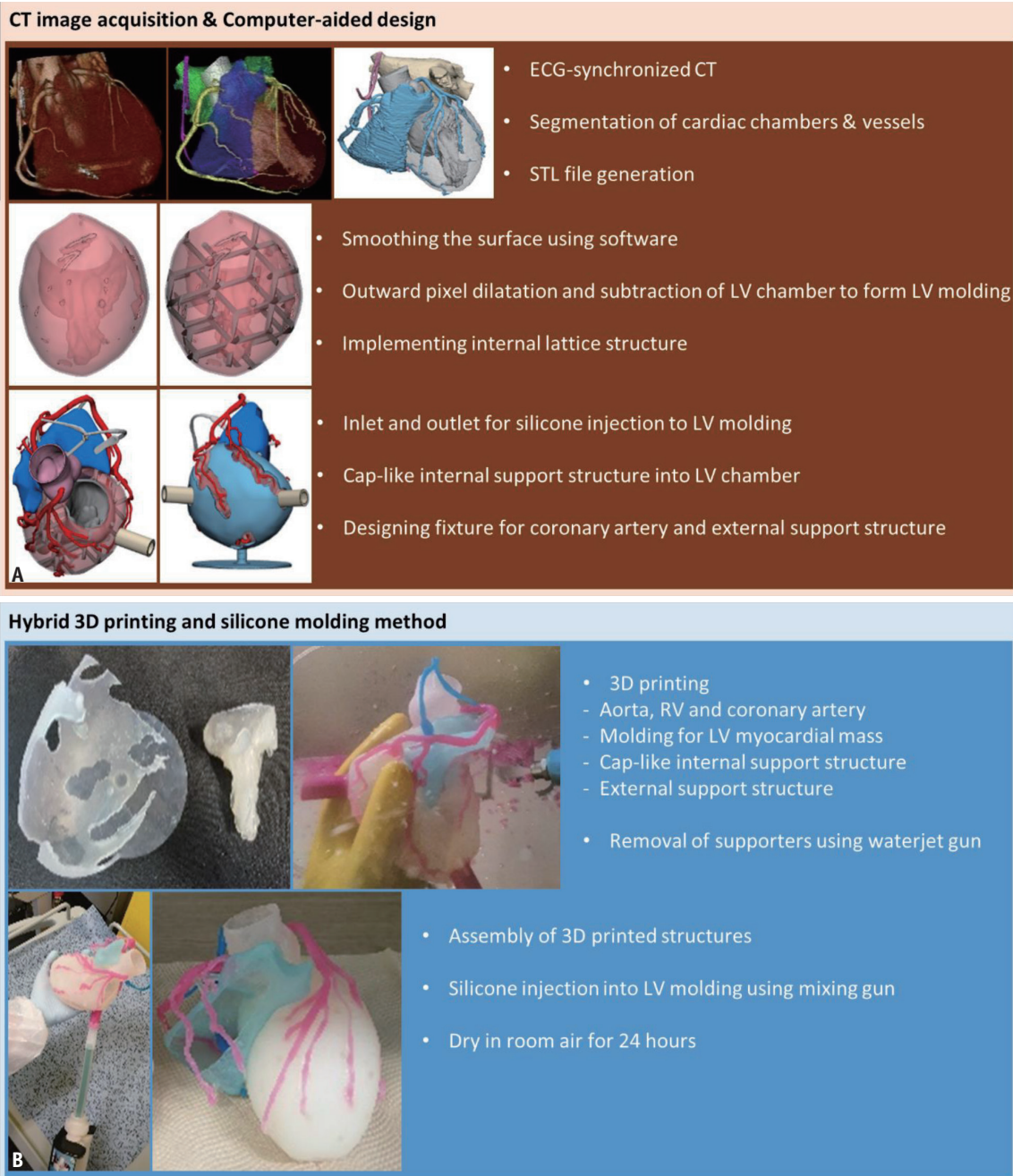


Fig. 1. The development of the resectable myocardial model using 3D printing was divided into two stages.

A. First, ECG-gated CT was performed, and the end-diastolic phase of the CT image was segmented into cardiac chambers and vessels to generate a STL file. The STL file was transferred to a computer-aided design, which included the additions of offsetting and contour, implementing support structures, and modeling of the inlet and outlet for silicone injection into the molding of the LV myocardial mass. **B.** Second, 3D printing of anatomic structures, such as the aorta, right ventricle, and coronary arteries, as well as the molding of the LV myocardial mass and the internal and external support structures, were performed. After assembling the 3D printouts, silicone was injected into the LV molding using an injection gun, followed by a drying process that lasted 24 hours. ECG = electrocardiography, LV = left ventricular, STL = standard tessellation language, 3D = three-dimensional

chamber, LV myocardial mass, LV chamber, right ventricular (RV) chamber, and aorta.

To equalize the uneven surface of the voxel cube-based CT image, a smoothing function of the software was

applied. The virtual LV endocardial and epicardial walls were generated by outward pixel dilatation and subtracting the origin chamber to design the molding for silicone injection. To prevent structural distortion during silicone injection of

the molding for the LV myocardial mass, the internal lattice structure of the LV myocardial mass and external support structures of the LV myocardial wall were implemented with emptying of the epicardial space where the 3D-printed blood vessels would be located. An inlet and an outlet for silicone injection were added to the LV myocardial mold at the base and apex of the myocardial model, respectively. The fixture for the coronary artery along the external surface of the LV mold was also added.

In addition, with inward pixel subtraction of the LV chamber, an internally supporting cap-like structure into the LV chamber was designed to further strengthen structural stability.

Hybrid 3D Printing and Silicone Molding Method

The process of hybrid 3D printing and silicone molding is summarized in Figure 1B. 3D printing was performed for the key structures, such as the aorta, coronary arteries, and RV chamber, using a 3D printer (Objet 500; TangoPlus FullCure resin; Stratasys Ltd.). In addition, to frame the cast for the silicone injection, the LV myocardial mass was printed in the form of a mold using the same 3D printer. The supporters that surrounded the inner and outer surfaces of the model to secure the printout during the printing process were removed using a waterjet gun. The cap-like internal support structure and external support structure were printed with another 3D printer using a more rigid material (Form 2; Formlabs). After assembling the 3D-printed anatomic structures, 3D-printed LV myocardial molding, and internal and external support structures, soft silicone (Ecoflex0010; Smooth-On Inc.) was injected into the assembled molding. The outputs were dried for 24 hours as the final step of the process.

CT Acquisition of the Myocardial Model and Wall Thickness Measurement

For patient 2 and patient 3, the CT of the myocardial model was performed with the model in the standard anatomical position using the same scan parameters that were applied for the cardiac CT. After mounting the source data in the image reconstruction software (Aquarius iNtuition viewer; TeraRecon Inc.), the CT data were reconstructed on short- and long-axis views to measure the thickness of the myocardial wall and the volumes of the LV cavity and myocardial mass based on the 17-segment American Heart Association model [22]. The measurements of myocardial wall thickness and volume using CT of the

myocardial model were compared with those measured by cardiac CT.

Mock Surgery Using a 3D Myocardial Model

Within a week before surgery, a mock septal myectomy was performed using the myocardial model by a heart surgeon with more than 20 years of experience in heart surgery assisted by a resident in major cardiothoracic surgery who attended as the first assistant during the actual surgery. With the known density of the silicone material (1.04 g/mL), the volume and weight of the resected silicone during mock surgery were measured [23].

Surgical Techniques of Transapical Myectomy

In brief, a standard median sternotomy was performed, and the heart was arrested using antegrade cardioplegia. The apex of the heart was delivered anteriorly. The left ventriculostomy was performed laterally to, and far enough from, the left anterior descending coronary artery to prevent its compromise during ventriculostomy site closure. The surgeon identified and protected the anterolateral and posteromedial papillary muscles and began myectomy on the ventricular septum to enlarge the LV cavity. The adequacy of myectomy was not only determined visually and by palpation, but also by measuring the weight and volume of resected myocardium and comparing these measured values with the accepted myocardial tissue density value (1.055 g/mL) [24].

Postoperative Complications and Follow-Up

The patients were followed-up for 3 postoperative months. The recommended assessments included chest radiography, physical examination, and transthoracic echocardiography. Postoperative complications and early outcomes, such as symptomatic improvement, were recorded. The follow-up study was carried out by subsequent clinic visits to outpatient departments.

RESULTS

Baseline Characteristics

The baseline clinical variables of the three ApHCM patients are shown in Table 1. All patients had NYHA class III/IV heart failure symptoms. The mean diastolic septal thickness and end-diastolic volume measured on echocardiography were 16 mm (range, 15–17 mm) and 105.3 mL (range, 87–124), respectively. Mid-ventricular

Table 1. The Clinical Characteristics of the Enrolled Apical Hypertrophic Cardiomyopathy Patients

	Patient 1	Patient 2	Patient 3
Age, years	73	75	56
Sex	Male	Male	Male
Preoperative findings			
NYHA classification	IV	III	III
Cardiothoracic ratio	0.73	0.64	0.56
Preoperative echocardiography			
LV internal diameter, mm			
End-systolic	15	38	21
End-diastolic	35	60	37
Ventricular septal thickness, mm			
Systolic	20	18	20
Diastolic	15	16	17
End-systolic volume, mL	27	26	45
End-diastolic volume, mL	79	75	95
Midventricular obstruction	(+)	(-)	(+)
Flow acceleration, m/sec	3.6	(-)	3.7
Apical aneurysm	(+)	(-)	(+)
Ejection fraction	66	65	53
Valvular abnormality	(-)	MR	(-)
Extent of Surgery			
	Transaortic and Transapical Extended Septal Myectomy	MV Repair and Transapical Myectomy	Transapical Myectomy
Postoperative findings			
Complications	None	None	None
NYHA classification	II	I	I
Cardiothoracic ratio	0.65	0.51	0.57
Postoperative echocardiography			
LV internal diameter, mm			
End-systolic	35	38	25
End-diastolic	52	58	39
Ventricular septal thickness, mm			
Systolic	11	13	19
Diastolic	9	8	17
End-systolic volume, mL	44	54	42
End-diastolic volume, mL	87	124	105
Midventricular obstruction	(-)	(-)	(+)
Flow acceleration, m/sec	(-)	(-)	2.0
Apical aneurysm	(-)	(-)	(-)
Ejection fraction, %	49	56	60

LV = left ventricular, MR = mitral regurgitation, MV = mitral valve, NYHA = New York Heart Association

obstruction and apical aneurysm, which suggest myocardial burn-out, were observed in patients 1 and 3. In patient 2, midventricular obstruction of the LV cavity was not observed because mitral regurgitation during systole allowed for a sufficient end-diastolic volume.

Mock Transapical Myectomy Using a Myocardial Model

The surgeon determined the optimal incision site that

was lateral and far enough from the left anterior descending artery to avoid coronary injury during the closure of the ventriculotomy site. The silicon material constituting the model was soft enough to be resected with a surgical blade. During and after the mock surgery, the surgeon could freely evaluate the adequacy of the muscle excision by visually and manually scrutinizing the myocardial model. The consistency of the surgical technique details of the mock

and real operations are presented in the Supplementary Movie 1. For patient 1, the degree of transapical resection seemed insufficient to relieve the obstruction of the LV outflow tract during the mock surgery; therefore, transaortic resection was planned and performed (Fig. 2). The volume of the resected silicone during the mock surgery was 6 mL (6.2 g in weight) and 12 mL (12.5 g in weight) for patients 2 and 3, respectively.

Comparison of Myocardial Thickness and Volume of the LV Chamber between CT of the 3D Model and Cardiac CT

The mean difference in the myocardial thickness obtained using preoperative CT and the myocardial model was low in the basal (0.3 mm) and mid-ventricular (1.0 mm) segments. However, the mean difference in the myocardial thickness was high in the apical segments (6.9 mm) and the apex (7.3 mm) (Fig. 3) (Table 2). The mean difference between the volume of the LV mass and the cavity was higher in the



Fig. 2. Representative photographs show the transaortic (A) and transapical (B) approaches simulated during mock surgery using a myocardial model. Intraoperative photographs show the surgeon's view during transaortic resection (C) and transapical resection (D) the finally resected specimens using each approach for patient 1. Photographs captured from the intraoperative arterial waveform monitor of the radial arterial line before (E) and after (F) myectomy show increased area under the curve of the arterial waveform after surgery, which may reflect improved stroke volume. AV = aortic valve

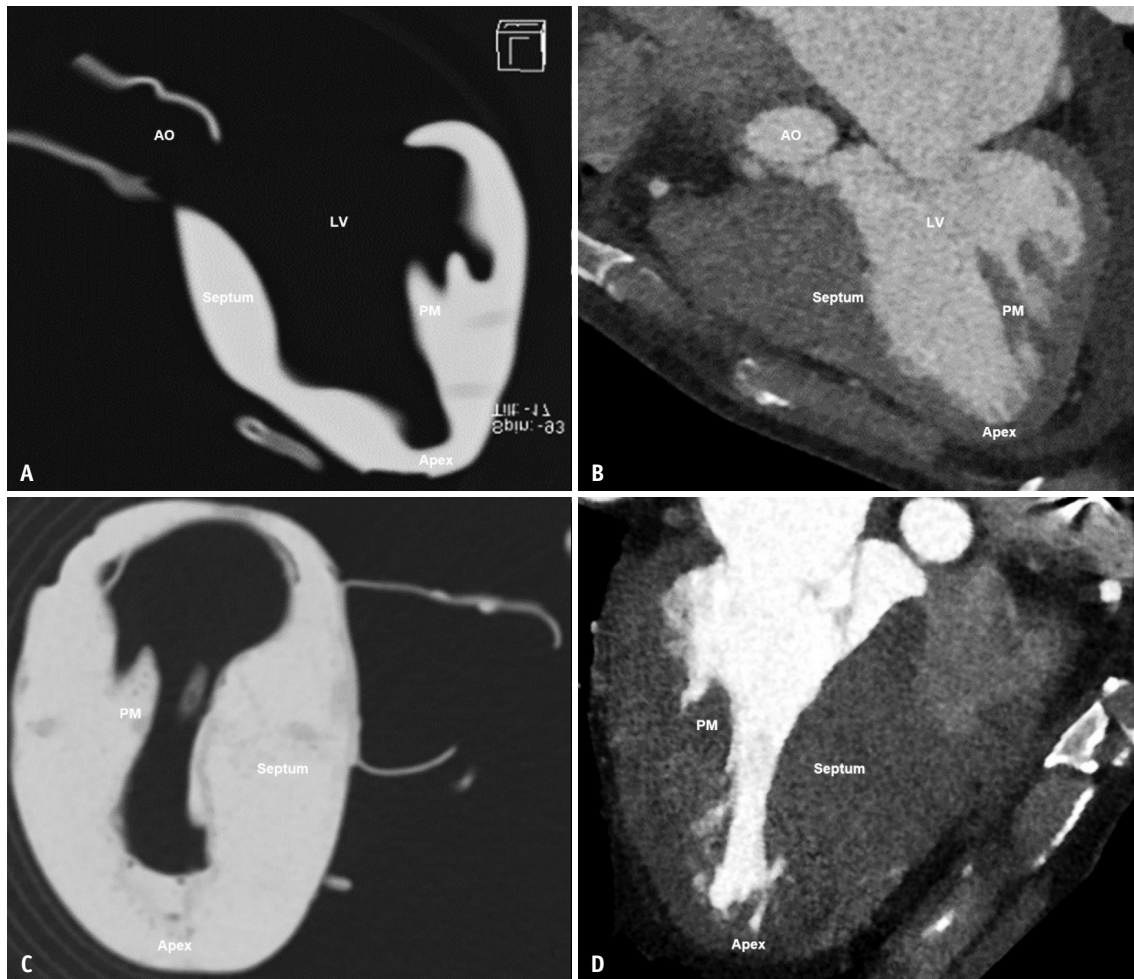


Fig. 3. Representative CT images obtained from the myocardial model (A, C) verify the structural consistency of the myocardial model compared with that of the cardiac CT images (B, D) of patient 2 and patient 3. However, the apical segments and the apex of the myocardial model of patient 3 were relatively thicker than those shown by cardiac CT (C). AO = aorta, LV = left ventricle, PM = papillary muscle

basal segments (36.9 mL and 14.8 mL, respectively) than in the mid-ventricular (2.9 mL and -9.4 mL, respectively) and apical segments (6.0 mL and -3.0 mL, respectively).

Surgical Procedure and Outcome after Transapical Myectomy

To enlarge the LV cavity, septal myectomy was performed via a transapical incision in all three cases. However, as planned during the mock surgery, the range of septal resection was extended to the heart base to relieve subaortic obstruction with a trans-aortic approach in patient 1. The amount of resected myocardium in patient 1 was 15 g and 27 g using the trans-aortic and trans-apical approaches, respectively (Fig. 2).

The actual volumes of resected myocardium were 5 mL (5.3 g in weight) and 11.2 mL (11.8 g in weight) for patient

2 and patient 3, respectively; this was comparable to the volume and weight of silicone during mock surgery (Figs. 4, 5). All three patients showed symptomatic improvements after surgery without postoperative complications (Table 1). The end-diastolic volumes improved from 79 mL (patient 1), 75 mL (patient 2), and 95 mL (patient 3) to 87 mL, 124 mL, and 105 mL, respectively.

DISCUSSION

The major finding of our study was that our new 3D myocardial model, which accurately reflects the anatomical details of the heart, was soft enough to facilitate surgical rehearsal. Furthermore, we reliably compared the results of mock surgery with those of the postoperative outcomes of myectomy based on the resected volumes and

Table 2. Mean Myocardial Thickness in Each Myocardial Segment and Mean LV Mass Volume Measured via Myocardial Model CT and Cardiac CT

	Cardiac CT (A)	Myocardial Model (B)	Difference (B-A)
Myocardial thickness, mm			
Basal			
Anteroseptal	13.1	12.7	-0.4
Inferoseptal	8.4	8.4	0.0
Inferior	10.0	12.9	2.9
Anterolateral	11.9	11.4	-0.5
Inferolateral	8.4	8.4	0.0
Anterior	18.2	18.1	-0.2
Mean difference	-	-	0.3
Midventricular			
Anteroseptal	21.0	20.5	-0.5
Inferoseptal	16.7	20.2	3.5
Inferior	14.7	17.2	2.5
Anterolateral	18.5	18.4	-0.1
Inferolateral	17.5	19.1	1.6
Anterior	21.7	20.5	-1.2
Mean difference	-	-	1.0
Apical			
Anterior	14.7	22.5	7.8
Septal	16.8	20.5	3.8
Inferior	8.1	13.4	5.3
Lateral	10.1	20.7	10.6
Mean difference	-	-	6.9
Apex	5.3	12.6	7.3
Volume, mL			
Basal			
LV mass	44.1	81.0	36.9
Cavity	49.7	64.5	14.8
Midventricular			
LV mass	119.3	122.2	2.9
Cavity	34.8	25.3	-9.4
Apical			
LV mass	85.8	91.8	6.0
Cavity	10.1	7.1	-3.0

LV = left ventricular

weights of the silicone material and myocardium; we also confirmed the clinical, radiographic, and echocardiographic improvements.

Novelty of Our 3D Model-Hybrid 3D Printing and Silicone Molding Method

Although several groups have implemented 3D printing for cardiovascular surgery, most previously reported 3D models have enabled only preoperative planning and virtual

simulation without manipulations meaningful to surgeons [12-15,25,26]. This may partially result from the current technical limitations of 3D printing or materials used for 3D printing in terms of securing anatomic details while enabling surgically meaningful manipulation. Similarly, in our previous report, we outlined the development of a 3D-printed model for extended septal myectomy guidance for obstructive HCM. The surgeon could only disassemble the myocardial model without surgically meaningful simulation because the 3D-printed thick septal myocardial mass was too hard to allow excision with a surgical blade, even when it was printed with the softest available material [18]. In this study, we attempted to overcome this limitation using the novel approach of hybridizing the 3D printing technique and silicone molding to secure anatomic details and reproduce a physically resectable LV myocardial mass.

Value of CT Acquisition of the Myocardial Model

We performed CT of the 3D myocardial model to verify the structural consistency between the model and its corresponding cardiac CT. The measured thickness and volume of the model were mostly consistent with those of cardiac CT. However, the silicone wall thickness in the apical portion of the heart was significantly enlarged with a difference of more than 5 mm. This difference may be attributable to the insufficient removal of the supporting material along the heart apex because of its deep innermost location and dense trabeculation along the endocardial surface of the cardiac apex. From these differences, we learned that in the deepest and innermost part of the 3D myocardial model, the supporting material should be removed meticulously with great caution. Regarding the volume measurement of the LV chamber and myocardial mass, the volume of the LV mass and cavity was higher in the basal segments (36.9 mL and 14.8 mL, respectively) than in the mid-ventricular (2.9 mL and -9.4 mL, respectively) and apical segments (6.0 mL and -3.0 mL, respectively). This may have resulted from the direction of the silicone material injection from the inlet to the outlet at the apex of the myocardial model because the force applied during silicone injection may have been stronger at the base. To overcome this limitation, we are now developing a silicone molding technique that would be more resilient to deformation, but this method is limited in terms of the detailed reproduction of separate anatomic structures, such as the coronary arteries [27]. Further

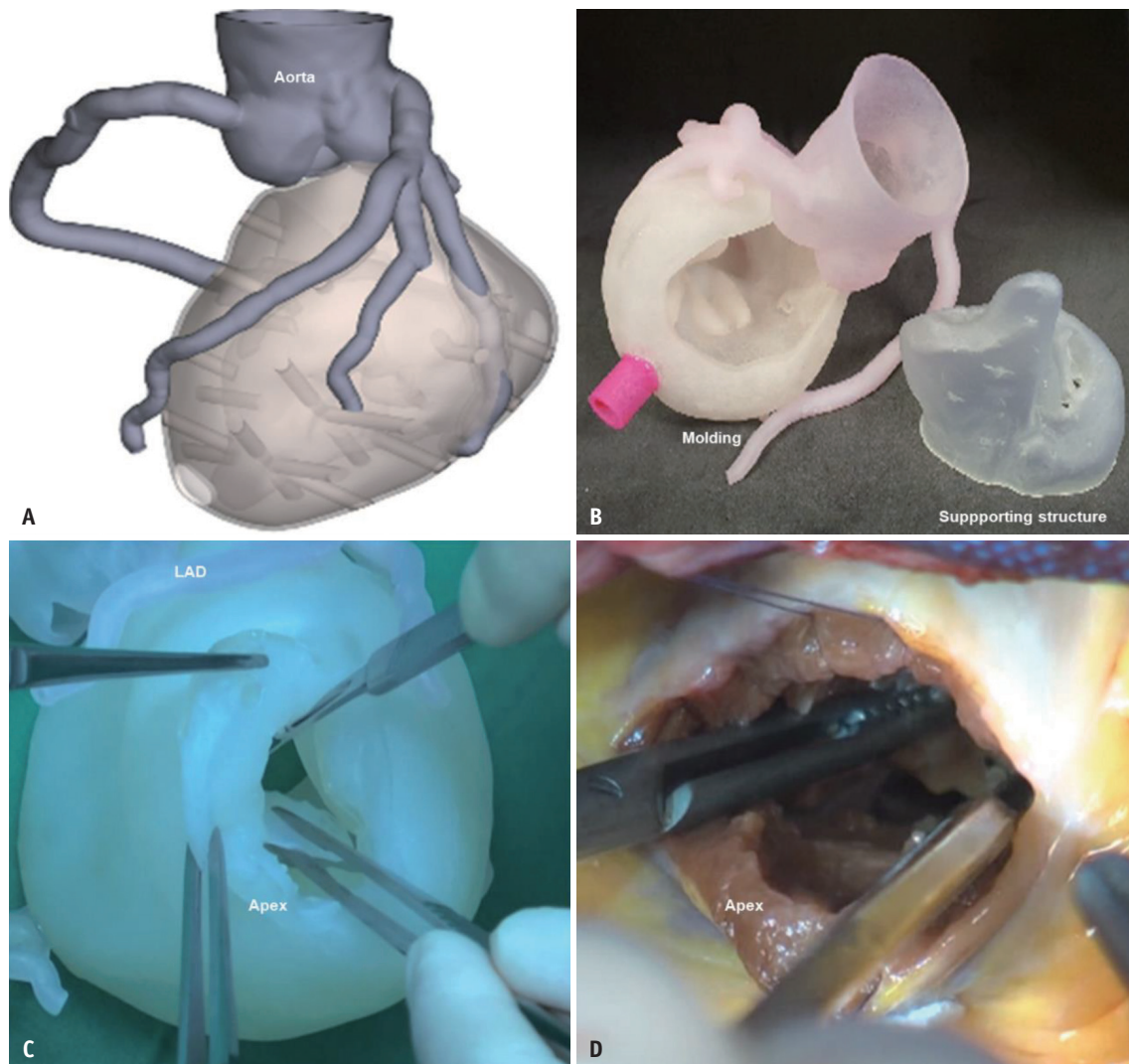


Fig. 4. Representative images from the STL file generated for patient 2 show the LV myocardial mass and its internal support structure, aorta, and coronary arteries (A). Based on this STL file, three-dimensional printing of anatomic structures, support structures, and molding for the LV myocardial mass were performed (B). After silicone injection into the LV mold followed by a drying process, a mock transapical myectomy was performed, and the anatomic relationship between the cardiac apex and coronary artery was demonstrated in the photograph (C). Intraoperative photography via the transapical approach shows the limited visual field of the LV cavity (D). LAD = left anterior descending artery, LV = left ventricular, STL = standard tessellation language

investigations to improve structural consistency should be carried out.

Clinical Implications

Transapical myectomy for apical HCM has been reported as an effective surgical option for increasing LV stroke volume among patients with small LV cavities and nonobstructive HCM. However, to the best of our knowledge, such reports have been consistently published by single institutions, suggesting that this procedure is not currently widely applied [4,28-30]. Furthermore, the transapical approach could be even more disadvantageous

than the classic transaortic approach because of a limited surgical field of view via ventriculostomy and the risk of inadequate resection, which may not allow for symptomatic improvement or excessive resection and can lead to damage to the mitral valves, complete heart block, or ventricular septal defects. To overcome these difficulties, we decided to apply patient-specific 3D printing surgical models to inform transapical myectomy for managing medically intractable ApHCM.

With our resectable 3D model, the surgeon could intuitively recognize essential details affecting transapical myectomy, such as the incision site for ventriculostomy

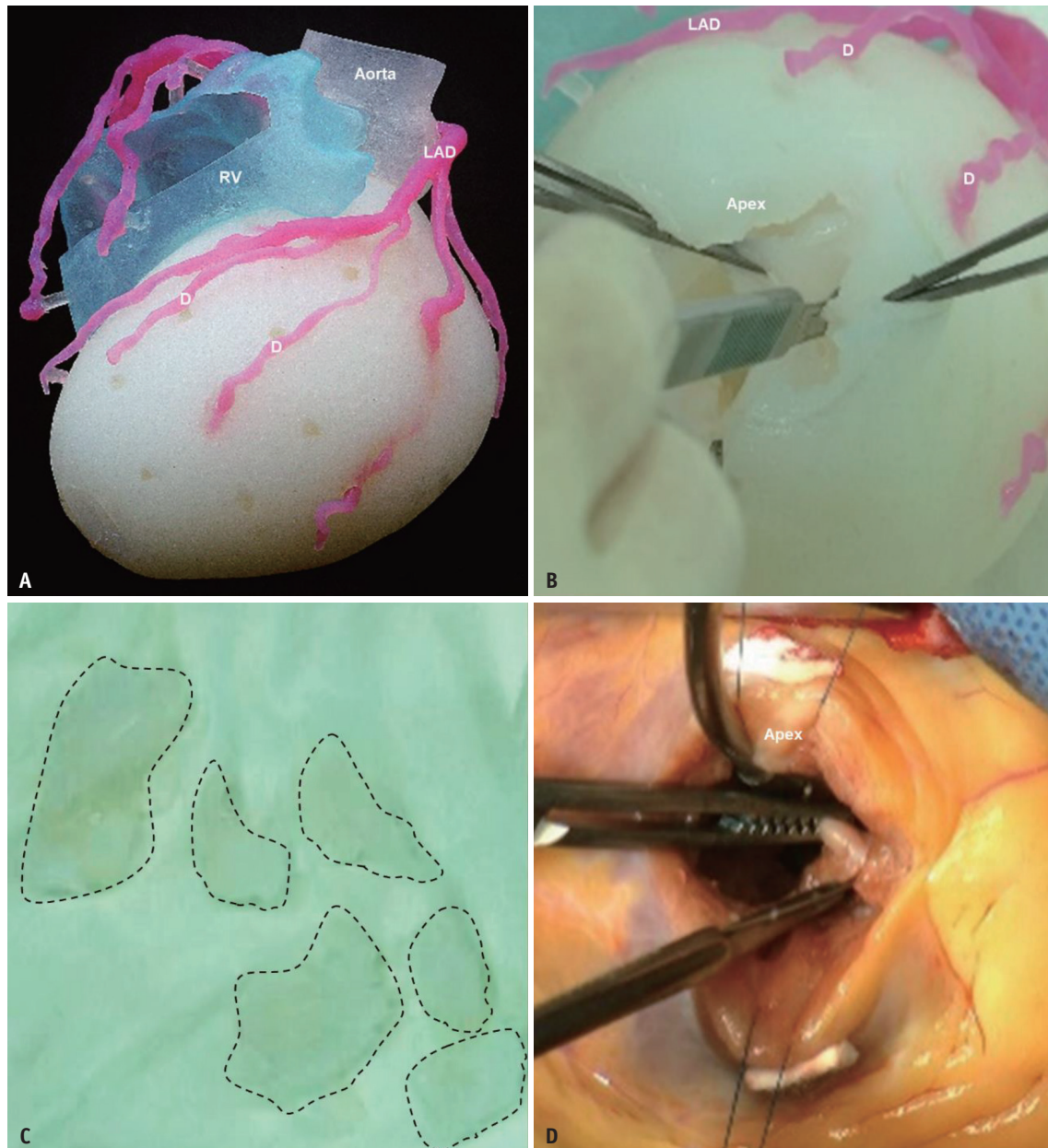


Fig. 5. Representative photograph shows the myocardial model of patient 3 using hybrid three-dimensional printing and silicone molding (A). A mock transapical myectomy was performed (B), and the excised pieces of silicone were outlined within the dotted line (C). Intraoperative photography obtained during transapical myectomy show a similar field of view compared with that of mock surgery (D). D = diagonal branch, LAD = left anterior descending artery, RV = right ventricle

and the location of papillary muscles. In this scheme, the 3D-printed mold was constructed on a 1:1 scale, which allowed surgeons to practice surgical rehearsal from the transapical perspective. Furthermore, the 3D-printed model could be freely rotated for observation from any angle, which helped in the design of individualized surgical plans, according to different hypertrophic interventricular septum phenotypes. This allowed preoperative planning for the transaortic and transapical approaches for patient 1. With

the known densities of the myocardium and the material used for 3D model production, we can optimize the extent of myectomy, which helps in verifying the appropriate extent of resection during surgery. Therefore, our study is noteworthy for heart surgeons who are less experienced with the transapical approach to septal myectomy. In addition, as there is an unmet need related to rendering CT images as 3D printed models capable of not only providing detailed anatomic information but also enabling mock

surgery, radiologists should, at a minimum, be familiar with developing 3D printing models for surgical practice.

Study Limitations

Our study had some limitations. First, our preliminary study included a few cases with missing data, such as CT measurements and the volume and weight of resected silicone for patient 1. Second, 3D printing with silicone injection into a printed mold requires a time-intensive workflow, and it is highly costly. Third, we did not perform CT of the myocardial models after mock surgery, which may have provided further information for determining the optimal extent of silicone resection. At our institution, we have set up post-mock surgery CT imaging as a routine protocol following transapical myectomy as a treatment for ApHCM.

In conclusion, our 3D model with hybrid 3D printing and silicone molding may be useful for determining the appropriate extent of resection and enabling precisely planned surgery guided by a rehearsal platform for ApHCM.

Supplement

The Supplement is available with this article at <https://doi.org/10.3348/kjr.2020.1164>.

Supplementary Movie Legends

Movie 1. The surgical technique details of the mock and real operations for patient 3.

Conflicts of Interest

Dong Hyun Yang hold stock in Anymedi Inc. (<http://anymedi.com/>). All other authors declare no conflict of interest.

Author Contributions

Conceptualization: Dong Hyun Yang, Wooil Kim. Data curation: Dong Hyun Yang, Joon-Won Kang, Hyun Jung Koo, Sung-Ho Jung. Formal analysis: Dong Hyun Yang, Wooil Kim, Minje Lim, You Joung Jang. Funding acquisition: Dong Hyun Yang. Investigation: Dong Hyun Yang, Wooil Kim, Minje Lim, You Joung Jang. Methodology: Dong Hyun Yang, Wooil Kim, Minje Lim, You Joung Jang. Project administration: Dong Hyun Yang, Wooil Kim. Resources: Dong Hyun Yang. Software: Dong Hyun Yang, Wooil Kim, Minje Lim, You Joung Jang. Supervision: Dong Hyun Yang, Joon-Won Kang, Hyun Jung Koo, Sung-Ho Jung. Validation:

Dong Hyun Yang, Joon-Won Kang, Hyun Jung Koo, Sung-Ho Jung. Visualization: Dong Hyun Yang, Wooil Kim, Minje Lim, You Joung Jang. Writing—original draft: Dong Hyun Yang, Wooil Kim, Minje Lim, You Joung Jang. Writing—review & editing: all authors.

ORCID iDs

Wooil Kim

<https://orcid.org/0000-0002-9743-7449>

Minje Lim

<https://orcid.org/0000-0001-9312-1319>

You Joung Jang

<https://orcid.org/0000-0003-3661-5923>

Hyun Jung Koo

<https://orcid.org/0000-0001-5640-3835>

Joon-Won Kang

<https://orcid.org/0000-0001-6478-0390>

Sung-Ho Jung

<https://orcid.org/0000-0002-3699-0312>

Dong Hyun Yang

<https://orcid.org/0000-0001-5477-558X>

REFERENCES

1. Baxi AJ, Restrepo CS, Vargas D, Marmol-Velez A, Ocazonez D, Murillo H. Hypertrophic cardiomyopathy from A to Z: genetics, pathophysiology, imaging, and management. *Radiographics* 2016;36:335-354
2. Klarich KW, Attenhofer Jost CH, Binder J, Connolly HM, Scott CG, Freeman WK, et al. Risk of death in long-term follow-up of patients with apical hypertrophic cardiomyopathy. *Am J Cardiol* 2013;111:1784-1791
3. Towe EC, Bos JM, Ommen SR, Gersh BJ, Ackerman MJ. Genotype-phenotype correlations in apical variant hypertrophic cardiomyopathy. *Congenit Heart Dis* 2015;10:E139-E145
4. Kunkala MR, Schaff HV, Nishimura RA, Abel MD, Sorajja P, Dearani JA, et al. Transapical approach to myectomy for midventricular obstruction in hypertrophic cardiomyopathy. *Ann Thorac Surg* 2013;96:564-570
5. Kim H, Park JH, Won KB, Yoon HJ, Park HS, Cho YK, et al. Significance of apical cavity obliteration in apical hypertrophic cardiomyopathy. *Heart* 2016;102:1215-1220
6. Hang D, Schaff HV, Ommen SR, Dearani JA, Nishimura RA. Combined transaortic and transapical approach to septal myectomy in patients with complex hypertrophic cardiomyopathy. *J Thorac Cardiovasc Surg* 2018;155:2096-2102
7. Tang Y, Song Y, Duan F, Deng L, Ran J, Gao G, et al. Extended myectomy for hypertrophic obstructive cardiomyopathy

- patients with midventricular obstruction. *Eur J Cardiothorac Surg* 2018;54:875-883
8. Nguyen A, Schaff HV, Nishimura RA, Geske JB, Dearani JA, King KS, et al. Apical myectomy for patients with hypertrophic cardiomyopathy and advanced heart failure. *J Thorac Cardiovasc Surg* 2019 Apr [Epub]. <https://doi.org/10.1016/j.jtcvs.2019.03.088>
 9. Maron MS, Rowin EJ, Olivotto I, Casey SA, Arretini A, Tomberli B, et al. Contemporary natural history and management of nonobstructive hypertrophic cardiomyopathy. *J Am Coll Cardiol* 2016;67:1399-1409
 10. Parachuri VR, Adhyapak SM. The case for surgical myectomy in hypertrophic cardiomyopathy: is strategic planning the key to success? *J Thorac Cardiovasc Surg* 2017;154:1687-1688
 11. Vukicevic M, Mosadegh B, Min JK, Little SH. Cardiac 3D printing and its future directions. *JACC Cardiovasc Imaging* 2017;10:171-184
 12. Sodian R, Weber S, Markert M, Loeff M, Lueth T, Weis FC, et al. Pediatric cardiac transplantation: three-dimensional printing of anatomic models for surgical planning of heart transplantation in patients with univentricular heart. *J Thorac Cardiovasc Surg* 2008;136:1098-1099
 13. Yang DH, Park SH, Kim N, Choi ES, Kwon BS, Park CS, et al. Incremental value of 3D printing in the preoperative planning of complex congenital heart disease surgery. *JACC Cardiovasc Imaging* 2020 Aug [Epub]. <https://doi.org/10.1016/j.jcmg.2020.06.024>
 14. Kiraly L, Tofeig M, Jha NK, Talo H. Three-dimensional printed prototypes refine the anatomy of post-modified Norwood-1 complex aortic arch obstruction and allow presurgical simulation of the repair. *Interact Cardiovasc Thorac Surg* 2016;22:238-240
 15. Guo HC, Wang Y, Dai J, Ren CW, Li JH, Lai YQ. Application of 3D printing in the surgical planning of hypertrophic obstructive cardiomyopathy and physician-patient communication: a preliminary study. *J Thorac Dis* 2018;10:867-873
 16. Hermsen JL, Burke TM, Seslar SP, Owens DS, Ripley BA, Mokadam NA, et al. Scan, plan, print, practice, perform: development and use of a patient-specific 3-dimensional printed model in adult cardiac surgery. *J Thorac Cardiovasc Surg* 2017;153:132-140
 17. Shiraishi I, Yamagishi M, Hamaoka K, Fukuzawa M, Yagihara T. Simulative operation on congenital heart disease using rubber-like urethane stereolithographic biomodels based on 3D datasets of multislice computed tomography. *Eur J Cardiothorac Surg* 2010;37:302-306
 18. Yang DH, Kang JW, Kim N, Song JK, Lee JW, Lim TH. Myocardial 3-dimensional printing for septal myectomy guidance in a patient with obstructive hypertrophic cardiomyopathy. *Circulation* 2015;132:300-301
 19. Gregory S, Timms D, Pearcy MJ, Tansley G. A naturally shaped silicone ventricle evaluated in a mock circulation loop: a preliminary study. *J Med Eng Technol* 2009;33:185-191
 20. Russo M, Koenigshofer M, Stoiber M, Werner P, Gross C, Kocher A, et al. Advanced three-dimensionally engineered simulation model for aortic valve and proximal aorta procedures. *Interact Cardiovasc Thorac Surg* 2020;30:887-895
 21. Lezhnev AA, Ryabtsev DV, Hamanturov DB, Barskiy VI, Yatsyk SP. Silicone models of the aortic root to plan and simulate interventions. *Interact Cardiovasc Thorac Surg* 2020;31:204-209
 22. Cerqueira MD, Weissman NJ, Dilsizian V, Jacobs AK, Kaul S, Laskey WK, et al. Standardized myocardial segmentation and nomenclature for tomographic imaging of the heart. A statement for healthcare professionals from the Cardiac Imaging Committee of the Council on Clinical Cardiology of the American Heart Association. *Circulation* 2002;105:539-542
 23. Smooth-On, Inc. Ecoflex™ 00-10. Smooth-on Web site. <https://www.smooth-on.com/products/ecoflex-00-10/>. Accessed September 22, 2020
 24. Gheorghe AG, Fuchs A, Jacobsen C, Kofoed KF, Møgelvang R, Lynnerup N, et al. Cardiac left ventricular myocardial tissue density, evaluated by computed tomography and autopsy. *BMC Med Imaging* 2019;19:29
 25. Farooqi KM, Saeed O, Zaidi A, Sanz J, Nielsen JC, Hsu DT, et al. 3D printing to guide ventricular assist device placement in adults with congenital heart disease and heart failure. *JACC Heart Fail* 2016;4:301-311
 26. Jacobs S, Grunert R, Mohr FW, Falk V. 3D-imaging of cardiac structures using 3D heart models for planning in heart surgery: a preliminary study. *Interact Cardiovasc Thorac Surg* 2008;7:6-9
 27. Chung P, Heller JA, Etemadi M, Ottoson PE, Liu JA, Rand L, et al. Rapid and low-cost prototyping of medical devices using 3D printed molds for liquid injection molding. *J Vis Exp* 2014;88:e51745
 28. Thompson AJ, Dearani JA, Johnson JN, Schaff HV, Towe EC, Palfreeman J, et al. What is the role of apical ventriculotomy in children and young adults with hypertrophic cardiomyopathy? *Congenit Heart Dis* 2018;13:617-623
 29. Kotkar KD, Said SM, Dearani JA, Schaff HV. Hypertrophic obstructive cardiomyopathy: the Mayo Clinic experience. *Ann Cardiothorac Surg* 2017;6:329-336
 30. Said SM, Schaff HV, Abel MD, Dearani JA. Transapical approach for apical myectomy and relief of midventricular obstruction in hypertrophic cardiomyopathy. *J Card Surg* 2012;27:443-448